Transmission eigenchannels in a disordered medium

Wonjun Choi,[1] Allard P. Mosk,[2] Q-Han Park,[1] and Wonshik Choi[1]
[1]*Department of Physics, Korea University, Seoul 136-701, Korea*
[2]*Complex Photonic Systems, Faculty of Science and Technology, and MESA + Institute for Nanotechnology, University of Twente, P.O. Box 217, 7500 AE Enschede, The Netherlands*
(Received 25 November 2010; revised manuscript received 3 March 2011; published 27 April 2011)

While the distribution of the transmission eigenvalues of a disordered medium is well understood in the context of random-matrix theory, the properties of eigenchannels have remained unexplored. In this study, we have solved electromagnetic wave propagation through a disordered medium using the finite-difference time-domain method, we numerically constructed a transmission matrix in an optical regime, and we obtained its eigenchannels as well as its eigenvalues. We observe that open eigenchannels enhance the energy stored inside the disordered medium. From mode decomposition, we prove that eigenchannels contribute to a single-channel optimizing mode, which is realized in recent experiments by I. M. Vellekoop *et al.* [Phys. Rev. Lett **101**, 120601 (2008)], in proportion to their eigenvalues. Our study will pave the way for experimental approaches to finding open eigenchannels and their potential use for imaging through turbid media and random lasers.

DOI: 10.1103/PhysRevB.83.134207 PACS number(s): 05.60.−k, 42.25.Dd, 73.23.−b

I. INTRODUCTION

The wave nature of light transport through highly scattering media offers many opportunities that are not present in diffusion theory. The effect of interference, a key aspect of the wave nature, has brought about many interesting phenomena, such as lasing in a mirrorless scattering medium and coherent backscattering.[1–3] With the recent advances of the wavefront shaping and phase recording technologies, the effects that were demonstrated in a conductor, ultrasound, and microwave studies have been realized in the optical regime. Among them are focusing beyond the diffraction limit, imaging through strongly scattering media, and enhanced transmission through coupling to the open eigenchannels.[4–7] In these studies, the so-called transmission matrix, which is the input-output relation of a given disordered medium for a basis of orthonormal channels, has played a major role. Once it is measured, the disordered medium is no longer a random object, and the output can be deterministically correlated with the input.[8] This transmission matrix can be directly measured by recording the output for each possible input, or it can be indirectly deduced by means of feedback or optical phase conjugation.[7,9]

The eigenvalues of a transmission matrix are not completely random even for randomly selected disordered media. As Dorokhov first derived in 1984 using random-matrix theory, the eigenvalue distribution has the shape of a hyperbolic secant function.[10] We refer to Dorokhov's approach as the random-matrix theory (RMT) throughout this paper.[11,12] A striking consequence of RMT is that there always exist "open eigenchannels" whose eigenvalues are unity, which means that these modes have perfect transmission. The existence of open eigenchannels was noticed earlier in the study of the conductance fluctuation in electron transport[13] and the fluctuation in total transmission,[14] and more recently in the experimental study of an optimizing single output channel in optics.[4] But the direct implementation of open eigenchannels is still an unresolved issue. This would require the full control of all possible input and output channels, which is unfortunately limited in the experiment by the finite numerical aperture of the detection system and the data-acquisition time.[6] The propagation behavior of eigenchannels within the medium, an interesting subject that remains unexplored, is even harder to investigate in the experiment. This would require an experimental method to probe the field inside the medium in addition to the experimental realization of eigenchannels. Also, it is difficult in the optical experiments to implement waveguide geometry that the analytical theory has assumed. Experimental studies have been performed so far in open slab geometry in which the eigenvalue distribution may deviate from what RMT predicts due to innate edge effects. Although the effect of defects is known to degrade the universality,[15] the validity of the analytic theory for open slab geometry is yet to be characterized.

In this study, we numerically construct a transmission matrix in the optical regime by solving the Maxwell equation using the finite-difference time-domain (FDTD) method.[16] We cover all the possible input channels to map a complete transmission matrix. By making a singular value decomposition, we obtain eigenchannels and eigenvalues of a transmission matrix, and we investigate the validity of analytic theory for open slab geometry. Through the decomposition of single-channel optimizing modes into eigenchannels, we prove that eigenchannels contribute to such optimizing modes in proportion to their eigenvalues. Finally, by calculating the propagation of eigenchannels inside the medium, we explore how each eigenchannel stores its energy within the disordered medium.

II. CONSTRUCT A TRANSMISSION MATRIX USING THE FDTD METHOD

To construct a transmission matrix for a disordered medium in open slab geometry, we numerically solve Maxwell equations by performing FDTD calculations. We prepare a two-dimensional disordered medium in the x-z plane [Fig. 1(a)]. To generate a disorder, absorption-free square particles with a side length of 200 nm and a fixed refractive index, n_p, are spatially distributed in a random manner in the vacuum. The fill factor is $50 \pm 0.5\%$. The configuration is equivalent to the

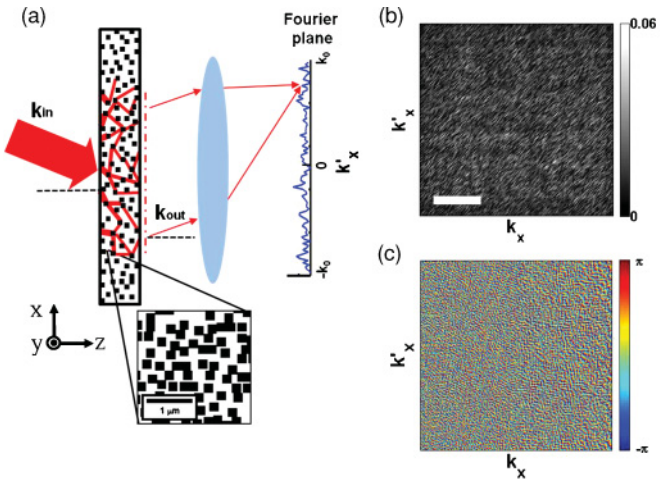

FIG. 1. (Color online) Construct a transmission matrix of a disordered medium. (a) Schematic of numerical simulation. The disordered medium is 130 μm wide in the x direction. The electric field is recorded at the output side of the medium indicated as a red dashed-dotted line and then numerically Fourier transformed to obtain the field at the wave-vector space, $k_{\text{out}} = (k'_x, k'_z)$. The lens represents numerical Fourier transform. The inset is the magnified image of the disordered medium. Black squares are the square particles. (b) and (c) Amplitude and phase of the transmission matrix. $k_x/2\pi$ and $k\prime_x/2\pi$ are covered from $-1/\lambda$ to $1/\lambda$. Scale bar: 5.1 μm^{-1} in k space. Color bar in (b) indicates the amplitude normalized to the amplitude of a normally incident input wave. Color bar in (c) indicates the phase in radians.

random array of dielectric rods extending along the y direction. At $n_p = 2.0$, which corresponds to the refractive index of zinc oxide, the scattering mean free path of the sample is calculated to be 372.6 $\pm$ 16.5 nm. We calculate the energy of the unscattered wave with respect to that of the incident wave as a function of slab thickness and find the scattering length from the exponential fitting.[17] Since it is impossible to prepare an infinitely wide sample in the numerical calculation, we initially prepare a wider sample than necessary and choose the center part of the output for the analysis. Specifically, the vertical width of the disordered medium in the x direction is set as 130 μm for the computation, but the output field is recorded at the 90 μm width in the middle (red dashed-dotted line). Disordered media of various slab thickness l_{th} in the z direction and refractive index n_p are considered as samples. A numerical cell size in the FDTD calculation is set to be 10 nm, which is sufficiently smaller than the wavelength, to ensure the accuracy of the computation.

We send a continuous wave of a planar wavefront and compute the field distribution inside and outside of the random medium until a steady state is established, which typically takes 1500 periods of optical oscillation. The light source is set to have a wavelength $\lambda = 600$ nm with input polarization orthogonal to the x-z plane (TE polarization mode). A set of the wave vector of an incident wave, $k_{\text{in}} = (k_x, k_z)$, is chosen in such a way as to form a complete basis. Since the width of a sample is set as $L = 90$ μm, those incident wave vectors whose k_x satisfies the relation $k_x/2\pi = m\Delta k = m/L$ with $-k_0 \leqslant k_x \leqslant k_0$ are independent channels. Here m is an integer and $k_0/2\pi = 1/\lambda$. Therefore there are 299 independent channels for the given wavelength of 600 nm. The k_z component of k_{in} is determined by the relation $k_z = \sqrt{k_0^2 - k_x^2}$.

For a basis of plane waves constituting a complete set of input channels, we compute their propagation through a disordered medium. At the steady state, we record electric fields along a line parallel to the x axis, which is located 50 nm behind the medium indicated by a red dashed-dotted line in Fig. 1(a). Recording is done at four successive times with a time interval of $1/(4ck_0)$, one-quarter of optical oscillation. By applying a phase-shifting interferometry algorithm,[18] we extract the amplitude and phase of the transmitted electric field, $E_{\text{out}}(x, z = z_d)$. To use k space for a basis of the transmission matrix, we perform numerical Fourier transform of $E_{\text{out}}(x)$ and obtain the electric field in k space, $E_{\text{out}}(k'_x)$. This process is illustrated as an insertion of a virtual lens behind the medium, as shown in Fig. 1(a). Then, we construct a transmission matrix, $t(k'_x, k_x)$, by the following relation:

$$E_{\text{out}}(k'_x) = t(k'_x, k_x) E_{\text{in}}(k_x). \tag{1}$$

Note that k_x indicates the wave-vector component at the input plane and $k\prime_x$ at the output plane. Figures 1(b) and 1(c) show the amplitude and the phase of the transmission matrix for the disordered medium of $l_{\text{th}} = 16$ μm and $n_p = 2.0$. The dimension of the matrix is 299 $\times$ 299 as there are 299 independent channels. Highly randomized patterns are visible in both amplitude and phase components of the transmission matrix.

III. EIGENVALUE DISTRIBUTION

We compare the numerically calculated transmission matrix with RMT by studying the singular values of the matrix. We perform the singular value decomposition of the transmission matrix, t,

$$t = U\tau V, \tag{2}$$

where τ is a diagonal matrix with non-negative real numbers on the diagonal, which are called singular values. V and U are unitary matrices mapping the input channels (k_x) to eigenchannels and eigenchannels to output channels (k'_x), respectively. The square of a singular value, known as a transmission eigenvalue, corresponds to the intensity transmission coefficient of the eigenchannel. We prepare disordered media with $l_{\text{th}} = 8$, 12, and 16 μm for the same $n_p = 2.0$, and calculate their transmission matrices. For each medium, we plot eigenvalues after arranging them in descending order [solid red curves in Fig. 2(a)]. With the increase of thickness, the area under the curve is reduced and thus the average eigenvalue decreases. Considering that an arbitrary input is a random superposition of eigenchannels, this decrease in average eigenvalue agrees well with the reduction in total transmission. In accordance with RMT, there always exists an eigenchannel whose transmission is unity, which is called an open eigenchannel, regardless of the thickness. This is rather surprising because the existence of completely open eigenchannels is predicted only in the waveguide geometry in which the energy flux, or net current in electron transport along a wire, is strictly conserved. One thing to note is that there exist eigenchannels whose transmission

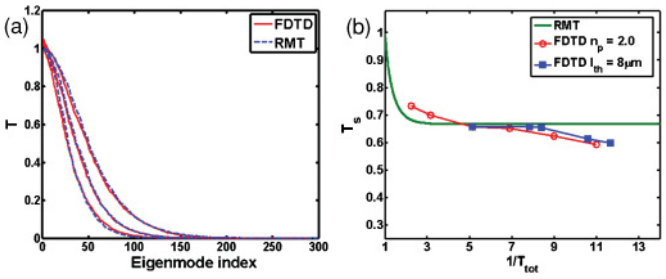

FIG. 2. (Color online) Comparison between FDTD computation and random matrix theory (RMT). (a) Eigenvalue distribution of the transmission matrix sorted in descending order. Red curves are calculated from the FDTD method while blue dashed curves are obtained by RMT. Three different curves account for three different disordered media with thicknesses of 8, 12, and 16 μm, respectively, for the same $n_p = 2.0$. For each of the FDTD results and RMT, the uppermost curve is from the 8 μm sample, the middle one is from the 12 μm sample, and the curve at the very bottom is from the 16 μm sample. (b) Transmittance of a single-channel optimizing mode, T_s. The green curve is the $C_{4,2}$ calculated from eigenvalues of RMT. A solid red curve with open circles is obtained from FDTD calculations at various thicknesses of media with the same index of particle $n_p = 2.0$. From left, the thicknesses are 2, 4, 8, 12, 16, and 20 μm, respectively. A solid blue curve with closed squares is acquired by the FDTD method for the same thickness of media with different indices of particles. From left, the index of particle is 2.0, 2.2, 2.23, 2.26, and 2.3, respectively.

slightly exceeds unity. This is due to the edge effect inevitable in the open slab geometry, which breaks the flux conservation. But the effect is rather mild and we can infer that the open slab geometry can be approximated by waveguide geometry for the studied media.

For a detailed comparison of the FDTD method with RMT, we plot the eigenvalue distribution derived by Dorokhov that satisfies the following relation:

$$\tau^2 = \sec h^2(\Gamma/2). \tag{3}$$

Here, Γ is a real diagonal matrix with non-negative real random numbers as its diagonal elements. In FDTD calculations, the total transmission of each sample varies due to the difference in thickness and the index of particles. Since the total transmission is related to the eigenvalues as $T_{\text{tot}} = \langle\tau^2\rangle$, where $\langle\rangle$ indicate an average operation, we set a maximum value, $\gamma_{\max}$, of the diagonal elements in Γ so as to match the total transmission, T_{tot}, of the medium considered in the FDTD calculations,[19]

$$\frac{\int_0^{\gamma_{\max}} \sec h^2(\gamma/2)d\gamma}{\gamma_{\max}} = T_{\text{tot}}. \tag{4}$$

The T_{tot} acquired from FDTD calculations for $l_{\text{th}} = 8$, 12, and 16 μm are 0.1924, 0.1444, and 0.1113, respectively. The values of $\gamma_{\max}$ that match the total transmission of the samples are 10.39, 13.85, and 17.97, respectively. For each of the samples, we construct a diagonal matrix Γ whose elements are randomly distributed between 0 and $\gamma_{\max}$, and obtain τ^2 by inserting the Γ into Eq. (3). The dashed blue curves in Fig. 2(a) show the eigenvalue distributions obtained from RMT. The distributions are in excellent agreement with our FDTD results. Moreover, this confirms that the open slab geometry of the given disordered media can be modeled by the RMT based on the waveguide geometry at least for the considered media.[15]

IV. SINGLE-CHANNEL OPTIMIZATION AND THE LIMITATION OF OPEN SLAB GEOMETRY

We numerically implement a so-called single-channel optimization that recent experiments have realized, and find that the transmission of the optimized modes provides a sensitive validation on whether the open slab geometry can be described by RMT. It was shown that the optimization of intensity at a certain output channel by a feedback control of input modes enhances the total transmission to 2/3 if the thickness of a medium is a few times larger than the transport mean free path.[4] For a given singular value distribution, the total transmission that this optimization process can achieve is known to be $C_{4,2} = \langle\tau^4\rangle/\langle\tau^2\rangle$ [Eq. (9) in Ref. 4]. The green curve in Fig. 2(b) shows the $C_{4,2}$ calculated from eigenvalues predicted by RMT [Eq. (3)] for disordered media of various total transmissions. This shows that the average eigenvalue of the RMT converges to the total transmission of 2/3 if the total transmission is smaller than 1/3, which is the case for opaque media, i.e., media thicker than a few mean free paths.

In our FDTD simulations, we perform a single-channel optimization process equivalent to the experimental procedure by controlling the amplitude and phase of input waves. By setting the amplitude of input waves at each channel as follows, we optimize the intensity at a particular output channel, k'_{x_opt}:[4]

$$E_{\text{in}}(k_x) = t^*(k'_{x\_\text{opt}}, k_x). \tag{5}$$

Here $*$ indicates a complex conjugate. By propagating this optimized input mode through a disordered medium, we obtain the transmitted field and its intensity. The open red circles in Fig. 2(b) are the total transmissions of the optimized input as a function of $1/T_{\text{tot}}$. We control T_{tot} by varying either the thickness or the index of particle of a disordered medium. We find that the transmittance converges to 2/3 up to $1/T_{\text{tot}} = 6.925$, but a further increase in $1/T_{\text{tot}}$ results in reduced transmittance. This turns out to be the edge effect of the open slab geometry. As the thickness increases, the field that leaks out of the analyzed windows becomes significant. We perform additional computations to confirm this point. While fixing the thickness of the media as 8 μm, we increase the index of particles. In doing so, the $1/T_{\text{tot}}$ is increased while the edge effect is regulated to a certain extent. As can be seen in square dots of Fig. 2(b), the transmission stays near 2/3 even with the increase of $1/T_{\text{tot}}$ until it reaches approximately 9. But the edge effect is revisited with the further increase in the particle index due to the increased scattering. Even if there are deviations of the open slab geometry from the waveguide geometry, the effect is rather mild until $1/T_{\text{tot}}$ reaches 12. In summary, we find that evaluation of the total transmission of single-channel optimization provides a sensitive measure of the condition in which the open slab geometry can be modeled as a waveguide geometry on which the random matrix theory is based. Our investigation suggests that the edge effect is negligible until the ratio between the thickness of the medium to the width of the sampling reaches 16 μm /90 μm = 0.18, as

long as the scattering mean free path is longer than 372.6 nm. This finding will be useful in determining the size of the sampling area in the experiment for the given thickness of a disordered medium.

V. CONTRIBUTION OF EIGENCHANNELS TO THE POINT-OPTIMIZING MODES

The single-channel optimizing process enhances total transmission to 2/3. This implies that eigenchannels with large eigenvalues preferentially contribute to an optimizing mode. As the eigenvalue has universal distribution and consequently the transmission of optimized modes has a unique number, that is 2/3, we expect that the contribution of each eigenchannel to the optimizing mode exhibits universality. In the FDTD method, we determine the contribution by decomposing the transmitted wave of an optimized mode into eigenchannels. Figure 3(a) shows a propagation of an optimizing wave through a disordered medium. Since we optimize an output channel of $k'_{x\_\mathrm{opt}} = 0$ in this case, the Fourier transform of the transmitted wave shows a sharp peak at the center [Figs. 3(b) and 3(c)]. The unitary matrix U, which maps an output channel to eigenchannels, is obtained from the singular value decomposition of the transmission matrix [Fig. 3(d)]. By projecting the optimized output mode [Fig. 3(c)] onto each column, say the xth column, of the U matrix, the contribution of the xth eigenchannel to the optimized mode, c_x, is obtained. Figure 3(e) shows the magnitude of c_x for all the eigenchannels. As expected, an eigenchannel with a larger eigenvalue (or smaller x) has a bigger contribution than that of the smaller eigenvalue. Notably, the distribution is similar to the eigenvalue distribution shown in Fig. 2. When overlapped with the eigenvalue distribution with a normalization factor that makes the area under the curve unity (solid blue curve), we find that they are indeed in excellent agreement. Therefore, we can deduce that the contribution of each eigenchannel to the optimizing mode is proportional to its eigenvalue.

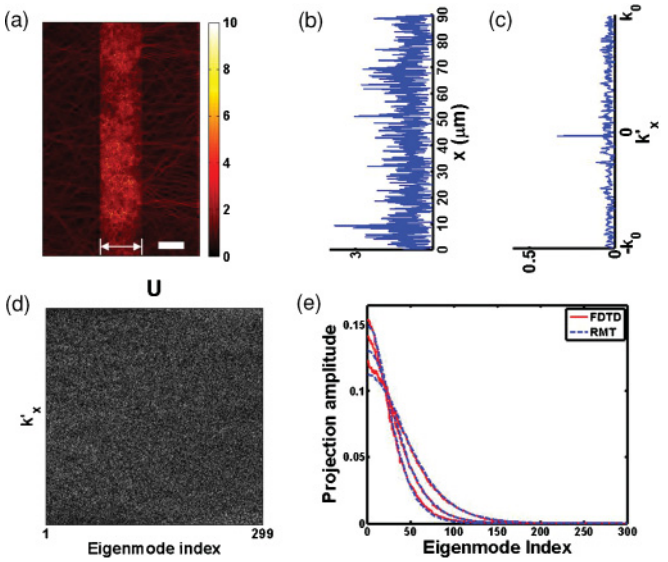

FIG. 3. (Color online) The propagation of the single-channel optimizing mode. (a) Field distribution inside and outside of a disordered medium. The light wave is incident from the left. The sample is located within the arrow indicated at the bottom. At the input side of the sample, the incident field is subtracted to exclusively visualize the reflection from the sample. The color bar indicates amplitude normalized to the input wave. Scale bar: 10 μm. (b) Amplitude profile of the field sampled at the output of the medium. (c) The spectrum of the output field obtained by taking Fourier transform of the field at the output. The intensity of the field is optimized at an output channel of $k'_x = 0$. (d) The amplitude of the U matrix mapping the eigenchannels to an output channel (k'_x). (e) The projection amplitude of the output field obtained by a single-channel optimizing mode (c) to each column of the U matrix. Red curves are $|c_x|$ acquired from FDTD calculation. Amplitudes are normalized to the input wave. The blue curves are the eigenvalue distribution predicted by RMT. It is normalized to make the area under the curve unity. Samples of 8, 12, and 16 μm thicknesses are investigated.

We analytically prove this proportionality in the following. Using Eq. (5), the transmitted wave of a single-channel optimizing mode is written as follows:

$$\tilde{E}_{k'_x} = \sum_{k_x} t(k'_x,k_x)E_{k_x} = A_0 \sum_{k_x} t(k'_x,k_x)t^*(k'_{x\_\mathrm{opt}},k_x). \qquad (6)$$

Projection of this transmitted wave onto the xth column of the unitary matrix U leads to the complex coefficient, c_x, representing the contribution of each eigenchannel to the optimizing mode,

$$c_x = \sum_{k'_x} U^*(k'_x,x)\tilde{E}_{k'_x} = A_0 U(k'_{x\_\mathrm{opt}},x)\tau^2_{xx}. \qquad (7)$$

We find that the ensemble average of $|c_x|$ is simply proportional to τ^2_{xx} by using the assumption of random matrix theory that $U(k'_{x\_\mathrm{opt}},x)$ and τ_{xx} are statistically independent. This perfectly explains our observation in FDTD calculations. Therefore, the single-channel optimization process puts weight on the open eigenchannels, and the increase of the total transmission of the optimized mode itself suggests the existence of the open eigenchannels.

VI. PROPAGATION OF EIGENCHANNELS IN A DISORDERED MEDIUM

The FDTD method differs from RMT in that it can provide the field distribution inside a disordered medium. This enables us to explore how eigenchannels propagate through the medium and how much energy they deposit into the medium. As a baseline, we first compute the propagation of a plane wave through a disordered medium whose thickness and index of particles are 16 μm and $n_p = 2.0$, respectively, and we obtain its field distribution both inside and outside of the medium (Fig. 4). The field amplitude throughout the medium is displayed in Fig. 4(a) when the incident angle is 11.5° with respect to the z axis. The incoming field is subtracted on the left-hand side of the disordered medium to exclusively visualize the reflected field by the medium. Inside the medium, there is a linear decrease in the amplitude of the field as the wave propagates through the medium, as is shown in Fig. 4(d), which plots the intensity averaged along the x axis as a function of the depth (z axis). This agrees well with previous studies[20,21] conducted in the context of diffusion theory in which the transmission decreases linearly when the

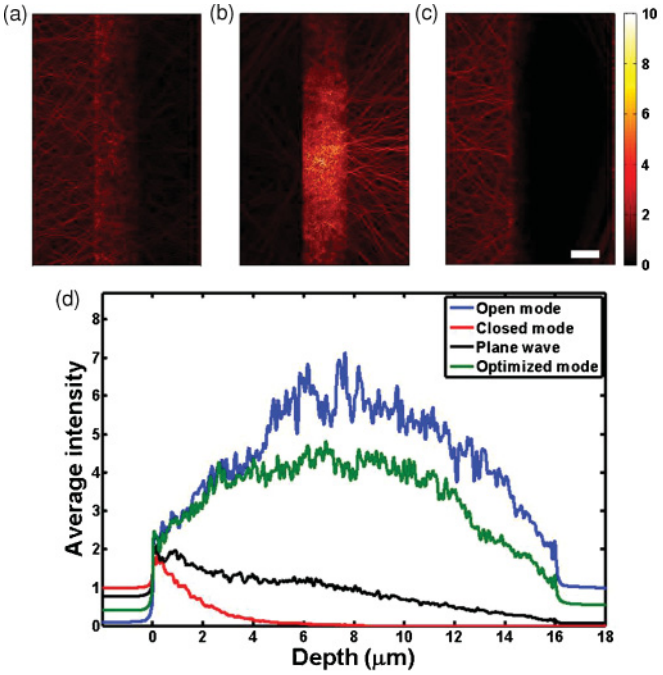

FIG. 4. (Color online) Field distributions of eigenchannels inside the medium. (a)–(c) Field distributions of a plane wave whose incident angle is 11.5°, open eigenchannel and closed eigenchannel, respectively. The incident field is subtracted on the left-hand side of the medium. Color bar: amplitude normalized to the input wave. Scale bar: 10 μm. (d) Average intensity along the x direction as a function of the depth in the z direction. The disordered medium fills the space between 0 and 16 μm in depth. The intensity is normalized to that of a normally incident plane wave.

thickness of the medium is much larger than the transport mean free path.

For the same disordered medium, we obtain eigenchannels from singular value decomposition of the transmission matrix, and we solve their propagation through the medium. Figure 4(b) displays the propagation of an open eigenchannel whose eigenvalue is 0.955. We find that the field strength inside the medium is enhanced such that its average intensity is higher than that of the input [blue curve in Fig. 4(d)]. This is in analogy with a Fabry-Perot cavity in which internal field strength increases at the resonance condition due to the constructive interference. Likewise, the constructive interference enhances the internal energy in open eigenchannels, which leads to strongly enhanced transmission. It is interesting to note that spatial mode coupling alone can enhance the field strength in the case of the disordered medium regardless of the source frequency. In the case of a closed mode whose eigenvalue is close to zero [Fig. 4(c)], a steep decrease of intensity is observed along the z direction as soon as the wave enters the medium. This suggests strong destructive interference as the wave reaches the end of the medium. The intensity profile follows the exponentially decaying curve [red curve in Fig. 4(d)]. Overall, the location of the peak intensity inside the medium shifts from the center to the input side with the decrease of the eigenvalue. The internal energy of the single-channel optimizing mode is close to the open eigenchannel in connection with its enhanced transmission.

Open eigenchannels in a passive medium may have a connection to photon diffusion in a medium with gain. As Payne and Yamilov have analyzed, the propagation profile has an enhanced peak in the middle of the medium when there is gain and it is exponentially decaying when there is absorption.[21] These profiles have some similarities with the open and closed eigenchannels of the passive medium, respectively. This may be due to the fact that the open eigenchannels preferentially elongate photon residence time, and gain in the photon diffusion emphasizes the importance of a very long light path.[22]

VII. CONCLUSION

In this study, we numerically explored the properties of eigenchannels in their field distribution inside a disordered medium and observed that open eigenchannels significantly enhance field energy in the medium in accordance with their high transmission. Furthermore, by constructing a transmission matrix in experimentally feasible open slab geometry with full coverage of input and output channels, we validate that the open slab geometry can still be modeled as waveguide geometry used in analytic theory as long as the thickness of the medium is 0.18 times smaller than the sampling width. Finally, we confirmed that the single-channel optimization process is equivalent to emphasizing the open eigenchannels. Our method will pave the way for an exploration of the experimental implementation of open eigenchannels and their potential use for imaging through turbid media and random lasers.

ACKNOWLEDGMENTS

This research was supported by the Basic Science Research Program through the National Research Foundation of Korea (NRF) funded by the Ministry of Education, Science and Technology (Grant No. 20100011286), by the Korea government (MEST) (No. 2010-0028713, 2010-0019171), and by a Korea University Grant.

[1]C. Vanneste, P. Sebbah, and H. Cao, Phys. Rev. Lett. **98**, 143902 (2007).
[2]J. Fallert, R. J. B. Dietz, J. Sartor, D. Schneider, C. Klingshirn, and H. Kalt, Nat. Photon. **3**, 279 (2009).
[3]P. E. Wolf, G. Maret, E. Akkermans, and R. Maynard, J. Phys. France **49**, 63 (1988).
[4]I. M. Vellekoop and A. P. Mosk, Phys. Rev. Lett. **101**, 120601 (2008).
[5]I. M. Vellekoop, A. Lagendijk, and A. P. Mosk, Nat. Photon. **4**, 320 (2010).
[6]S. M. Popoff, G. Lerosey, R. Carminati, M. Fink, A. C. Boccara, and S. Gigan, Phys. Rev. Lett. **104**, 100601 (2010).

[7]I. M. Vellekoop and A. P. Mosk, Opt. Lett. **32**, 2309 (2007).
[8]I. Freund, Physica A **168**, 49 (1990).
[9]Z. Yaqoob, D. Psaltis, M. S. Feld, and C. Yang, Nat. Photon. **2**, 110 (2008).
[10]O. N. Dorokhov, Solid State Commun. **51**, 381 (1984).
[11]M. L. Mehta, *Random Matrices*, 3rd ed. (Academic, London, 2004).
[12]A. Edelman and N. Raj Rao, Acta Numer. **14**, 233 (2005).
[13]S. Washburn, IBM J. Res. Dev. **32**, 335 (1988).
[14]J. F. de Boer, M. C. W. van Rossum, M. P. van Albada, T. M. Nieuwenhuizen, and A. Lagendijk, Phys. Rev. Lett. **73**, 2567 (1994).
[15]Y. V. Nazarov, Phys. Rev. Lett. **73**, 134 (1994).
[16]A. Taflove and S. C. Hagness, *Computational Electrodynamics. The Finite-Difference Time-Domain Method*, 3rd ed. (Artec House, Boston, 2005).
[17]E. J. McDowell, M. Cui, I. M. Vellekoop, V. Senekerimyan, Z. Yaqoob, and C. H. Yang, J. Biomed. Opt. **15**, 025004 (2010).
[18]K. Creath, Prog. Opt. **26**, 349 (1988).
[19]C. W. J. Beenakker, Rev. Mod. Phys. **69**, 731 (1997).
[20]J. G. Rivas, R. Sprik, C. M. Soukoulis, K. Busch, and A. Lagendijk, Europhys. Lett. **48**, 22 (1999).
[21]B. Payne, J. Andreasen, H. Cao, and A. Yamilov, Phys. Rev. B **82**, 104204 (2010).
[22]S. Mujumdar, M. Ricci, R. Torre, and D. S. Wiersma, Phys. Rev. Lett. **93**, 053903 (2004).